ISNN:2181-1296



SHAROF RASHIDOV NOMIDAGI
SAMARQAND DAVLAT UNIVERSITETI

САМАРКАНДСКИЙ ГОСУДАРСТВЕННЫЙ
УНИВЕРСИТЕТ ИМЕНИ ШАРОФА РАШИДОВА

SAMARKAND STATE UNIVERSITY NAMED
AFTER SHAROF RASHIDOV

ILMIY AXBOROTNOMA

НАУЧНЫЙ ВЕСТНИК
SCIENTIFIC JOURNAL

ANIQ VA TABIIY FANLAR SERIYASI

Matematika, Mexanika, Informatika
Fizika, Kimyo, Biologiya, Geografiya

№ 1/1 (155)
2026

ISSN 2181-1296

ILMIY AXBOROTNOMA

НАУЧНЫЙ ВЕСТНИК SCIENTIFIC JOURNAL

2026-yil, 1-son (155/1) ANIQ VA TABIIY FANLAR SERIYASI

Matematika, Mexanika, Informatika, Fizika, Kimyo, Biologiya, Geografiya

Samarqand viloyat matbuot boshqarmasida ro‘yxatdan o‘tish tartibi 09-25.
Jurnal 1999-yildan chop qilina boshlagan va OAK ro‘yxatiga kiritilgan.

BOSH MUHARRIR **R. I. XALMURADOV, t.f.d., professor**
BOSH MUHARRIR O‘RINBOSARLARI: **H.A. XUSHVAQTOV, f-m.f.d., dotsent**

TAHRIRIYAT KENGASHI:

Sh.A.Alimov	- O‘zFA akademigi	**M.X.Ashurov**	- O‘zFA akademigi
S.N.Lakayev	- O‘zFA akademigi (SamDU)	**B.J.Axmedov**	- O‘zFA akademigi
M.M.Kamilov	- O‘zFA akademigi	**Q.G‘.G‘ulomov**	- O‘zFA akademigi
A.G.Yagola	- Moskva davlat universiteti professori (Rossiya)	**A.A.Zaxidov**	-Texas Nanotexnologiya instituti professori (AQSh)
Alberto Del Bimbo	-Florensiya universiteti professori (Italiya)	**N.B. Ferapontov**	- Moskva davlat universiteti professori (Rossiya)
Sh.Tugizov	-Kaliforniya universiteti professori (AQSh)	**V.L.Popov**	-Berlin texnika universiteti professori (Germaniya)
A.S.Soleev	- f.-m.f.d., professor (SamDU)	**N.F.Bunkin**	- Moskva davlat texnika universiteti professori (Rossiya)
I.A.Ikromov	- f.-m.f.d., professor (SamDU)	**Haji Akber Aisa**	-Xinjiang tibbiyot universiteti professori (Xitoy)
B.X.Xo‘jayarov	- f.-m.f.d., professor (SamDU)	**E. A. Abduraxmonov**	- k.f.d., professor (SamDU)
L.Sabirov	-f.-m.f.d., professor (SamDU)	**N. K. Muxamadiyev**	- k.f.d., professor (SamDU)
A.Jumaboyev	-f.-m.f.d., professor (SamDU)	**L. A. Bulavin**	- Kiev milliy universiteti
X.Bozorov	-k.f.d., professor (SamDU)	**X. Q. Xaydarov**	- b.f.d., professor (SamDU)
O.Q.Quvondiqov	-f.-m.f.d. professor (SamDU)	**Z. I. Izzatullayev**	- b.f.d., professor (SamDU)
A.Z.Xasanov	-f.-m.f.d. professor (SamDU)	**A.B.Hasanov**	-tex.f.d., professor (SamDU)
Muhammad Suzuri bin Hitam	- Terengganu universiteti professori (Malayziya)	**Sh. T. Xoliqulov**	- q.-x.f.d., professor (SamDU)
K.D.Kuliyev	- f.-m.f .n. professor (SamDU)	**S. B. Abbosov**	- g.f.d., professor (SamDU)
A.M.Xolxo‘jayev	-f.-m.f.d., professor (SamDU)	**M.E. Mo‘minov**	-f.-m.f.d., professor (SamDU)
J.Abdullayev	-f.-m.f.d., professor (SamDU)	**I.I.Jumanov**	-tex.f.d., professor (SamDU)
A.R.Axatov	-tex.f.d., professor (SamDU)	**N.S.Mamatov**	-tex.f.d., professor (TIQXMMI)
D.B.Xursanov	- g.f.f.d., dotsent (SamDU)	**A.Sh.Yarmuxamedov**	-f-m.f.n., dotsent (SamDU)
F.Nazarov	-tex.f.d., dotsent (SamDU)	**X.S.Xaydarov**	-f-m.f.n., dotsent (SamDU)

Obuna indeksi – yakka tartibdagi obunachilar uchun **- 5583,**
tashkilot, korxonalar uchun **- 5584**

M U N D A R I J A
C O N T E N T S

№	Maqola nomi	Article title	Bet/ page
1.	$CsPbBr_3$ kvant nuqtalariga asoslangan lyuminissent quyosh konsentratorlarining optik xossalarini optimallashtirish **Nurimov A.D., Davurov Sh.M., Sherqulov E.S., Juraboyev L.A., Zakhidov A.**	Optimising optical performance of $CsPbBr_3$ quantum dots-based luminescent solar concentrators **Nurimov A.D., Davurov Sh.M., Sherqulov E.S., Juraboyev L.A., Zakhidov A.**	**5-10**
2.	Impuils-davriyli lazer nuri ta'sirida rux oksidi va rux selenid mikrokukunlarida uyg'otilgan fotolyuminesensiya **Rakhmatullaev I.A., Khaydarov Kh.S., Hoshimov Q.H., Abdusattorov B.A.**	Photoluminescence in zinc oxide and zinc selenide micropowders under pulsed-periodic laser excitation **Rakhmatullaev I.A., Khaydarov Kh.S., Hoshimov Q.H., Abdusattorov B.A.**	**11-15**
3.	Perovskit–polimer kompozitiga asoslangan ko'k bir qatlamli yorug'lik chiqaruvchi diodlar **Rahmonova M.O., Muxamadiyev N.Q.**	Blue single-layer light-emitting diodes based on a perovskite–polymer composite **Rahmonova M.O., Muxamadiyev N.Q.**	**16-23**
4.	Chegaraviy oqim bilan berilgan chiziqsiz diffuziya sistemasining sonli tadqiqoti **Yarmetova D.**	Numerical study of a nonlinear diffusion system with boundary fluxes **Yarmetova D.**	**24-28**
5.	Iqlim o'zgarishi sharoitida samarali haroratlar yig'indisi taqsimoti (Samarqand viloyati misolida) **Kholbaev G., Eshmirzaev D., Egamberdiev Kh., Shermukhammedov U., Arzikulov M., Yuldasheva Sh.**	Spectral properties of schrödinger operator for a two-fermion system on a lattice: eigenvalues and resonances **Kholbaev G., Eshmirzaev D., Egamberdiev Kh., Shermukhammedov U., Arzikulov M., Yuldasheva Sh.**	**29-36**
6.	Janus kinaza ingibitorlari sifatida 4,6-dialmashgan xinazolin hosilalarini dizayni va sintezi **Gaybullaev Sh., Takhirov Y., Zohidov K., Chao Niu, Bozorov Kh.**	Design and synthesis of 4,6-disubstituted quinazoline derivatives as janus kinase inhibitors **Gaybullaev Sh., Takhirov Y., Zohidov K., Chao Niu, Bozorov Kh.**	**37-43**
7.	Suzuki-miyaura usulida 3-almashingan-pirido[2,3-*d*]pirimidinonlarning sintezi **Khushnazarov Z., Turgunov D., Bozorov Kh.**	Synthesis of 3-substituted-pyrido[2,3-*d*]pyrimidinones by the suzuki-miyaura method **Khushnazarov Z., Turgunov D., Bozorov Kh.**	**44-48**
8.	2-metil-pirazolo[3,4-*d*]pirimidinonlarning sintezi **Ruzieva F., Turgunov D., Bozorov Kh.**	Synthesis of 2-methyl-pyrazolo[3,4-d]pyrimidinones **Ruzieva F., Turgunov D., Bozorov Kh.**	**49-53**
9.	Organo/noorganik ms-schiff gibrid sorbentning metall kationlariga nisbatan sorbsiya xossalarini baholash **Kuliboyeva N., Uzokov J., Mukhamadiyev A., Ruziyev I., Mukhamadiyev N.**	Evaluation of the sorption properties of organo/inorganic ms-schiff hybrid sorbents towards metal cations **Kuliboyeva N., Uzokov J., Mukhamadiyev A., Ruziyev I., Mukhamadiyev N.**	**54-64**

№	Maqola nomi	Article title	Bet/ page
10.	Qaror daraxtlariga asoslangan anjuman usullari yordamida ma'lumotlarni oldindan qayta ishlash va tasniflash algoritmlari **Akhatov A., Nazarov F.**	Data preprocessing and classification algorithms using ensemble methods based on decision trees **Akhatov A., Nazarov F.**	**65-74**
11.	Fotokatalitik faollikka ega TiO_2 nanoklasterlarini struktur va elektron xossalarini kvant kimyoviy usullarda baholash **Mamaziyayeva S., Uzokov J., Toshpulatova L., Mukhamadiyev N., Mukhamadiyeva Kh.**	Evaluation of the structure and electronic properties of photocatalytic tio2 nanoclusters using quantum chemical methods **Mamaziyayeva S., Uzokov J., Toshpulatova L., Mukhamadiev N., Mukhamadieva Kh.**	**75-81**
12.	Cu(II) ionlarining Piren sorbsiyasini sinergetik ta'sirini Langmuir-Freundlich modellashtirish asosida baholash **Vokhidov A., Kosimov S., Khalilov S., Mukhammadiyev N.**	Evaluation of the synergetic effect of pyrenee sorption of cu(ii) ions based on langmuir-freundlic modeling **Vokhidov A., Kosimov S., Khalilov S., Mukhammadiev N.**	**82-90**
13.	Magnit suyuqliklarining magneto-optik yorug'lik o'tkazuvchanligi **Kuvandiqov O., Kirgizov S., Mamasoliyev B., Kirgizova M.**	Evaluation of the synergetic effect of pyrenee sorption of cu(ii) ions based on langmuir-freundlic modeling **Kuvandikov O., Kirgizov S., Mamasoliev B., Kirgizova M.**	**91-97**
14.	Sun'iy intellekt mexanizmlari asosida suv tarkibini aqlli tahlil qilish usullari **Salimova M., Nazarov F.**	Methods for intelligent analysis of water composition based on artificial intelligence mechanisms **Salimova M., Nazarov F.**	**98-107**
15.	Glukoza asosida uglerodli kvant nuqtalarining fotolyuminestentsiya xossalari **Sobirova F., Ishankulov A., Khalilov K., Galyametdinov Y.**	Photoluminescence properties of glucose-based carbon quantum dots **Sobirova F., Ishankulov A., Khalilov K., Galyametdinov Y.**	**108-112**
16.	Bir o'lchamli kvadrat panjara zinasida diskret Shredinger operatorining xos qiymatlari **Muminov M.I., Sadullaeva M.S.**	On eigenvalues of the discrete schrödinger operator on a ladder of one-dimensional square lattice **Muminov M.I., Sadullaeva M.S.**	**113-120**
17.	O'zbekistonda aholi hududiy harakatining mintaqaviy xususuyatlari **Mukhamedov O.L.**	Regional characteristics of population territorial movement in Uzbekistan **Mukhamedov O.L.**	**121-126**

UDC: 620.3: 544.7 https://doi.org/10.59251/2181-3973.2025.v1.138.1. 3761

EVALUATION OF THE STRUCTURE AND ELECTRONIC PROPERTIES OF PHOTOCATALYTIC TiO2 NANOCLUSTERS USING QUANTUM CHEMICAL METHODS

S.Mamaziyaeva[1], J.Uzokov[1], L.Toshpulatova [1], N.Mukhamadiev[1], Kh.Mukhamadieva[2]

[1]Samarkand State University named after Sharof Rashidov, Samarkand, Uzbekistan.
[2] Secondary school No. 95 in Urgut district. Samarkand, Uzbekistan.

S.Mamaziyaeva Samarkand State University named after Sharof Rashidov, Samarkand, Uzbekistan.

Received: 16.01.2026
Revised: 25.01.2026
Accepted: 13.02.2026
Published: 30.03.2026

Publisher: Samarkand State University named after Sharof Rashidov.

Abstract. When the atomic number of $(TiO_2)_n$ clusters increases from 7 to 9, the energy of the forbidden region (lattice gap) and its size (wavelength) change (DFT) were calculated based on the B3LYP/6-31G** basis set. These values were found to be equal to the following. For n = 7, the forbidden region energy decreases to 3.5 eV, and when n = 9, the forbidden region energy decreases to 2.95 eV. This indicates that the lattice gap decreases and the photocatalytic activity increases with increasing atomic number in the clusters. Also, the electron localization function τ (r) (ELF) and η (r) and the localized orbital locator η (r) (localized orbital locator, LOL) representing the state of the bonding electron clouds in the nanoclusters were topologically analyzed. High ELF values (~0.8-1.0) indicate strongly localized electrons (e.g. lone pairs, bond regions, or core electrons), while low ELF values (~0-0.3) have been found to correspond to delocalized electrons (such as conjugated p-systems).

Keywords. Nanocluster, TD-DFT/ B3LYP/6-31G**, Hirshfeld 3D surface topography map, photocatalytic activity.

Fotokatalitik faollikka ega TiO_2 nanoklasterlarini struktur va elektron xossalarini kvant kimyoviy usullarda baholash

Annotatsiya. $(TiO_2)_n$ klasterlarida atom son qiymati 7 dan 9 gacha ortganda, taqiqlangan hudud (tarmoq bo‘shlig‘i) energiyasi va uning o‘lchamining (to‘lqin uzunligi) o‘zgarishi (DFT) B3LYP/6-31G** bazis to’plami asosida hisoblab topildi. Bu qiymatlar quyidagilarga teng ekanligi aniqlandi. n = 7 uchun taqiqlangan hudud energiyasi 3.5 eV ga, n = 9 ga yetganda, taqiqlangan hudud energiyasi 2.95 eV ga qadar kamayadi kuzatildi. Bu esa klasterlarda atom soni ortishi bilan tarmoq bo’shlig’ining kamayishi va fotokatalitik faolligi ortishini bildiradi. Shuningdek, nanoklasterlarda bog’lovchi elektron bulutlarning holatini ifodalaydigan elektron lokalizatsiya funktsiyasi τ (*r*) (electron localization function, ELF) va η (*r*) va lokallashgan (mahalliy) orbital lokatori η (*r*) (localized orbital locator, LOL) topologik tahlili amalga oshirildi. Yuqori ELF qiymatlari (~ 0,8-1,0) kuchli lokalizatsiya qilingan elektronlarni (masalan, yolg'iz juftliklar, bog'lanish hududlari yoki yadro elektronlari) ko'rsatadi, past ELF qiymatlari (~0-0,3) delokalizatsiyalangan elektronlarga (konyugatsiyalangan p-sistema kabi) mos kelishi aniqlandi.

Kalit so‘zlar. Nanoklaster, TD-DFT/ B3LYP/6-31G**, Hirshfeld 3D sirt topografik xaritasi, fotakatalitik faollik.

Оценка структурных и электронных свойств фотокаталитически активных нанокластеров TiO_2 с использованием квантово-химических методов

Аннотация. Энергия запрещенной зоны и ее размер (длина волны) изменяются в кластерах $(TiO_2)_n$ по мере увеличения атомного номера от 7 до 9 с использованием базисного набора (DFT) B3LYP/6-31G**. Полученные значения оказались равными следующим значениям. Для n = 7 энергия запрещенной зоны уменьшается до 3,5 эВ, а для n = 9 — до 2,95 эВ. Это указывает на то, что ширина запрещенной зоны уменьшается, а фотокаталитическая активность возрастает с увеличением атомного номера в кластерах. Также был проведен топологический анализ функций локализации электронов τ(r) (ELF) и η(r), а также локализованного орбитального локатора η(r) (локализованный орбитальный локатор, LOL), представляющих состояние связывающих электронных облаков в нанокластерах. Высокие значения ELF (~0,8-1,0) указывают на сильно локализованные электроны (например, неподеленные пары электронов, области связей или электроны внутренних оболочек), тогда как низкие значения ELF (~0-0,3) соответствуют делокализованным электронам (например, сопряженным p-системам).

Ключевые слова: нанокластер, TD-DFT/B3LYP/6-31G**, трехмерная топографическая карта поверхности Хиршфельда, фотокаталитическая активность.

Introduction. In recent years, there has been a significant increase in research on the synthesis of semiconductor nanoclusters with photocatalytic activity, their morphology and textural characteristics. Currently, there is increasing attention to the use of promising alternative semiconductor materials to traditional methods. These processes are relatively simple in terms of equipment requirements and are cost-effective. Photocatalytically active nanomaterials involve the generation of reactive species such as •OH radicals, which provide rapid and efficient oxidation of organic, inorganic and biological pollutants. Heterogeneous photocatalysis using oxide-based nanomaterials is particularly effective in the removal of water-soluble pollutants from water and wastewater under the influence of light [1-3].

Titanium dioxide (TiO_2) nanoparticles and composite materials based on them are among the most promising solutions, and TiO_2 has attracted much attention due to its important textural characteristics, such as low toxicity, biocompatibility, and wide band gap. TiO_2 nanoclusters are a class of nanomaterials with photocatalytic activity due to their high surface area and nanoscale pores. Therefore, TiO_2 clusters serve as an ideal model to study the catalytic properties of nanostructured TiO_2 for pollutant degradation in first-principles calculations. Qu and co-workers studied the structural and electronic properties of $(TiO_2)_n$ (n=1÷16) nanoclusters as a function of size using first-principles calculations. In these studies, the first step in fully understanding the catalytic mechanism of TiO_2 nanoclusters and in the studies based on it is to select appropriate structural models with relatively high stability and dimensions [5]. For example, in 2016, Arab et al. evaluated the structural stability of $(TiO_2)_n$ (n=1÷10) nanoclusters using a first-principles approach by analyzing their energetic properties, including binding energy, second-order energy difference, and dissociation energy [5-6].

TiO_2 nanoclusters have a hierarchical surface morphology and have been well studied and attracted attention due to their various physicochemical properties that can improve photocatalytic performance. This strategy has become one of the excellent ways to solve the problems related to the kinetic and thermodynamic aspects of TiO_2 photocatalysis. The hierarchical nanostructure design for TiO_2 has good molecular diffusion kinetics, improved absorption of irradiation light, increased surface area, and excellent charge carrier separation with less chance of recombination [7].

There are different phases of TiO_2, the most stable and widespread of which is rutile. Rutile occurs naturally and is used in industry for photocatalytic applications that do not require activation by sunlight. It has a high optical and mechanical density. The anatase phase of TiO_2 has stronger photocatalytic properties than rutile, and is therefore widely used in photocatalytic and self-cleaning coatings that operate under sunlight. Anatase is more commonly used in fine fibers and thin coatings.

Anatase is the phase with the highest photocatalytic activity, and the wide band gap value of both phases (3.0÷3.2 eV) leads to the activation of these materials under UV-VS light irradiation. In order to stabilize the photocatalytic process, it is necessary to develop materials that are highly photoreactive under sunlight. Considering that sunlight contains only 4÷5% of UV-VS radiation, it is necessary to find nanostructures with visible light absorption, which accounts for 50% of the solar spectrum. In order to achieve full photoactivation of this semiconductor under visible light irradiation, numerous modifications of TiO_2 at the nanoscale have been carried out. Composites obtained with non-metallic compounds have yielded partially positive results, since the red shift of the absorption edge of TiO_2, in turn, increases the recombination rate of the hole-electron pair. The creation of heterostructures based on TiO_2 combined with semiconductors with a low band gap can be an effective approach to improve the photocatalytic conversion of pollutants in water. The fundamentals of synthesis and photoactivation of TiO2 low-bandgap semiconductor heterostructures are studied, and some of the data on the photocatalytic activity of these materials are presented to shed light on their potential use for water purification. at a high scale [8-10].

Calculation methods. Quantum chemical calculations were performed on the stable structure of (TiO2)n (n=10÷50) nanoclusters. Calculation of the charge density distribution in the molecule for the optimized structure of the nanoclusters was performed using the semi-empirical (PM3), electrostatic potential, reactivity descriptors, and values of the stable energies using the density functional theory (DFT) Monte Carlo algorithm and the B3LYP/6-31G** basis set. The values of the HUMO and LUMO levels were obtained for easy access to the calculations of molecular orbital energies.

Results and their discussion. Quantum chemical calculations, including BLYP, B3LYP, and CAM-B3LYP DFT calculations, were performed on the optimized geometric structures of TiO2 nanoclusters (Fig. 1).

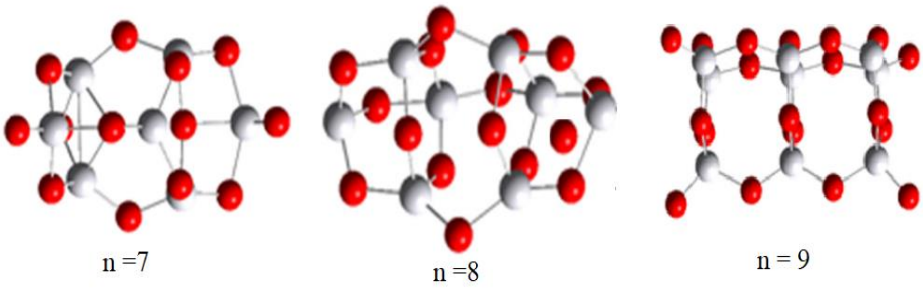

Figure 1. Optimized geometric structure of (TiO2)n (n =7; 8; 9) nanoclusters

Using the LANL2DZ basis set and semi-empirical PM3 methods, the calculated results show that the Ti-O bond length decreases with increasing number of atoms in the clusters. In particular, the Ti-O bond length in the n = 7 cluster is calculated to be 1.895 A°, 1.884 A° for n = 8, and around 1.825 A° for n = 9. From this, it can be concluded that the stability of the clusters increases with increasing number of atoms in TiO2 nanoclusters.

The vibrational binding energies of clusters with different structures were calculated using the DFT B3LYP/6-31G** basis set using the optimized geometry of the clusters. For clusters with $n \leq 7$, the singlet and triplet states are close to each other. It was observed that with increasing number of atoms in the clusters, the binding energies of atoms bound in the singlet state become higher than those in the triplet state [11]. This once again confirms that their stability increases with increasing number of atoms in the clusters. Quantum chemical analysis of $(TiO_2)_n$ nanoclusters shows that the structural and electronic properties vary significantly depending on the cluster size. Larger clusters reduce the enhanced stability and chemical reactivity due to changes in the total energy and band gap energy. These trends indicate that $(TiO_2)_n$ clusters, especially those with high atomic size, are of interest for practical applications requiring stable and conductive nanomaterials. The most important physical parameters of the clusters obtained based on (DFT) B3LYP/6-31G** calculations are presented in Table 1.

Table 1

Some physical parameters of $(TiO_2)n$ (n = 7 ÷ 9) clusters

$(TiO_2)_n$	Total energy *E*, (eV)	Chemical potential (eV)	Electrophile index (eV)	Dipole moment (Debye)
7	-235,5	-3,2	1,5	4,3
8	-477,3	-2,9	1,7	4,7
9	-716,5	-2,7	1,8	5,1

The increase in the total energy value of large clusters, which indicates their thermodynamic stability, helps such products to remain active in photocatalytic processes for a long time.

The Xirshfeld surface image (density surface) of the $(TiO_2)n$ cluster was studied using the Cristal Explorer 17 software. The Hirshfeld surface image provides an effective representation of the electron density and charge distribution. Image analysis is important for studying the electron distribution and polarization of clusters (Figure 2). The colors obtained from the surface analysis indicate the polarization on the surface. Green color indicates areas with neutral charge on the surface, yellow and red colors indicate areas with high electron density or partially negatively charged parts. Blue indicates areas with low electron density. It can be seen that the green color dominates in the 3D image obtained from the Hirshfield surface analysis. This indicates that the charge distribution in the $(TiO_2)_5$ cluster is almost the same. The red and yellow colors indicate the magnitude of the electron density concentrated around the electronegative element oxygen atom in the cluster.

The contribution of bonds that increase the stability of the crystal system from the Hirshfeld 3D surface topography map was calculated using the corresponding 2D fingerprint plot calculations using the CIF system input file. The outer boundary of the area occupied by a molecule or atom in a crystalline environment is called the Hirshfeld surface. For each location on the isosurface, two distances are defined in terms of dnorm: di - the distance to the nearest nucleus inside the surface and de - the distance to the nearest atoms outside the surface. The contribution of interactions between molecules is used to determine both distances. The normalized contact distance (dnorm) values, which depend on the de and di of the atom and its van der Waals (vdW) radii, were summarized in the equation. The Hirshfeld surface analysis is generated by dividing the intracrystal space by the ratio of the promolecule to the procrystal electron density by 0.5 and is depicted on the map using the normalized contact distance (d_{norm}) [12].

$$d_{norm} = \frac{d_i - r_i^{vdV}}{r_i^{vdV}} + \frac{d_e - r_e^{vdV}}{r_e^{vdV}} \quad (1)$$

(1) r_i^{vdV} va r_e^{vdV} are the van der Waals radii of the atoms corresponding to the inner and outer surfaces, respectively. The dnorm value is negative or positive depending on whether the intermolecular contacts are shorter or longer than the van der Waals separations. Contacts with a distance equal to the sum of the van der Waals radii are shown in white on the Hirshfeld 3D surface topography map, while contacts shorter and longer than the van der Waals radii are shown in red and blue, respectively.

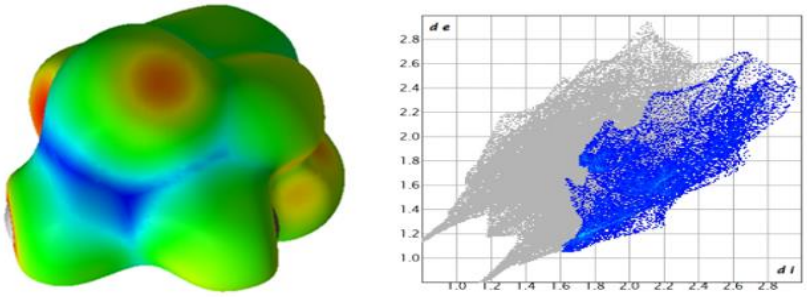

Figure 2. Hirshfeld surface image (a) and Hirshfeld fingerprints (b) of the $(TiO_2)_7$ cluster

In addition, reduced density gradient (RDG) analysis was performed to determine non-covalent interactions in nanocluster molecules, in particular Van der Waals interactions and intermolecular steric effects [13]. In the RDG analysis, the contribution of interactions through the electron density ρ(r) and its gradient |∇r(r)| was calculated as follows:

$$RDG(r) = \frac{1}{2(3\pi r^2)^{\frac{1}{3}}} \cdot \frac{|\nabla \rho(r)|}{\rho(r)^{\frac{4}{3}}}, (2)$$

In the equation, r is the electron density, and ∇ ρ(r) represents the average value of the electron density. By comparing ρ(r) with the value λ2, one can understand the nature and strength of the interactions present in the molecule. When the value of λ2 is λ2 < 0, interactions occur between atoms and functional groups in the molecule, while the value λ2 > 0 represents repulsive forces occurring in the molecules. A graph representing the proportion of non-covalent interactions in nanoclusters with different structures is presented in Figure 3.

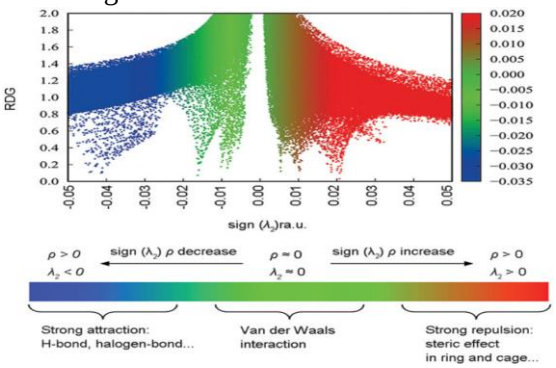

Figure 3. Reduced density gradient (RDG) map for $(TiO_2)_7$ nanocluster

The electron localization function (ELF) and η (r) and the localized orbital locator (LOL) representing the state of the bonding electron clouds in nanoclusters were topologically analyzed. ELF and LOL maps are advanced quantum chemical tools used to analyze the electronic structure at the molecular surface of the cluster [14-16]. Both methods provide information about chemical bonding, electron localization, and reactivity based on different aspects of the electron density and wave function. ELF and LOL are also used in chemical bonding classification and in investigating charge changes at the molecular surface. ELF and LOL offer similar interpretations, as they both depend on the kinetic energy density. LOL is usually seen when localized orbitals overlap and produces significant gradients of localized orbitals, and ELF, on the contrary, is calculated based on electron pair density.

High ELF values (~0.8÷1.0) indicate strongly localized electrons (such as lone pairs, bond regions, or core electrons), while low ELF values (~0-0.3) correspond to delocalized electrons (such as conjugated p-systems). The ELF value for periodic crystal systems by Savin via DFT is as follows:

$$x_\sigma(r) = \frac{2\left(\tau_\sigma(r) - \tau_\sigma^W(r)\right)}{\tau_\sigma^{LSDA}(r)} = \frac{\tau_\sigma^P(r)}{\tau_\sigma^{LSDA}(r)} \qquad (3)$$

$$ELF_\sigma = \frac{1}{1 + \chi_\sigma^2} \qquad (4)$$

The ELF maps for the $(TiO_2)_7$ nanocluster are presented in Figure 4. As the number of atoms increases, the photocatalytic activity of $(TiO_2)_n$ nanoclusters also increases, meaning that larger clusters are more efficient in photocatalytic processes than smaller ones. The main reasons for this are: first, increased energetic stability.

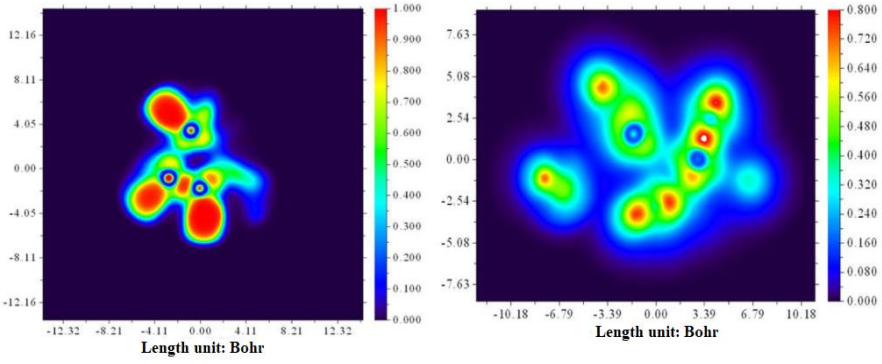

Figure 4. ELF and LOL maps for $(TiO_2)_7$ nanocluster

Clusters with many atoms have a higher total energy value, which helps them remain active in photocatalytic processes for a longer time. Second, decreased band gap energy: As the number of atoms increases, the band gap energy also changes. This is important for photocatalysis because when the band gap is small, the clusters can absorb more visible light. Increasing the light energy increases the photocatalytic activity and the process. HOMO and LUMO Energy (Figure 3 [17-18]). The distance between the HUMO (Highest Occupied Molecular Orbital) and LUMO (Lowest Unoccupied Molecular Orbital) energies decreases with increasing cluster size (n). This energy difference is called the band gap or band gap, and it is expressed in electron volts (eV) rather than in units of size (nm) [19,20]. In $(TiO_2)_n$ clusters, when the atomic number increases from 7 to 9, a change in the band gap energy and its size was observed. In nanoclusters (DFT), the band gap energy was calculated using the B3LYP/6-31G** basis set and was found to be equal to the following values. For n = 7, the band gap energy was 3.5 eV, and for n = 9, the band gap energy decreased to 2.95 eV.

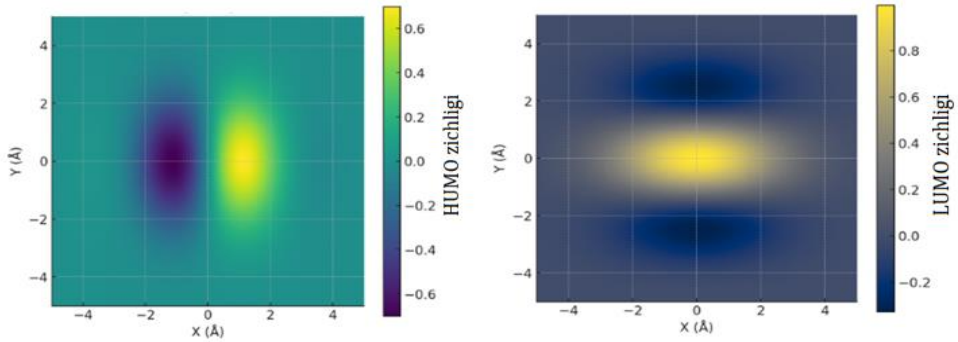

Figure 3. HOMO and LUMO molecular orbitals of (TiO2)7 nanoclusters

The wavelength corresponding to the band gap energy is calculated using Planck's constant λ and the speed of light. The wavelength (λ) of light corresponding to the band gap energy in a semiconductor can be calculated using the basic relationship between photon energy and Planck's constant (h).

$$E = h\nu \quad yoki \quad \lambda = \frac{h\,c}{E} \quad (5)$$

(5) In the equation $h = 6.626 \cdot 10^{-34}$ (J·s), Planck's constant, $c = 3.00 \cdot 110^{8}$ s is the speed of light in vacuum, E is the electron transition energy. This formula allows us to directly calculate the characteristic wavelength corresponding to the forbidden energy levels of clusters or other forbidden energy levels, and the electron transition energy directly relates the cluster structure to optical absorption.

Conclusion. In $(TiO_2)_n$ clusters, when the atomic number increases from 7 to 9, the change in the band gap energy and its size (wavelength) is found to be equal to the following values in the (DFT) B3LYP/6-31G** basis set. For n = 7, the band gap energy decreases to 3.5 eV, and when n = 9, the band gap energy decreases to 2.95 eV. This indicates that with the increase in the atomic number in the clusters, the band gap decreases and the photocatalytic activity increases.

References

1. Park H., Shin D. J., Yu J. Categorization of quantum dots, clusters, nanoclusters, and nanodots //Journal of Chemical Education. – 2021. – V. 98. – №. 3. – P. 703-709.
2. Uzokov J. Kosimov S., Muxamadiev A., Voxidov A., Mukhamadiev N., Anvarov T. Quantum chemical study of the photocatalytically active Mo-quercetin complex //Advanced Materials for Optics and Photonics: Chemistry and Engineering Perspectives (AMOP 2025). – SPIE, 2025. – V. 14014. – P. 117-124.
3. Hayitova M. Baxranova M., Uzokov J., Muxamadiev A., Mukhamadiev N., Khakimov F. Elemental composition, spectral characteristics, and quantum chemical insights into SRTIO3

perovoskite //Advanced Materials for Optics and Photonics: Chemistry and Engineering Perspectives (AMOP 2025). – SPIE, 2025. – V. 14014. – P. 90-96.
4. Uzokov J., Fayziyeva G., Mukhamadiev N., Ruziyev I., Kuliboyeva N., Saidov, K. Quantum chemical study of the photocatalytic activity Fe3O4/SiO2-trimesic acid-melamine supramolecular system //Advanced Materials for Optics and Photonics: Chemistry and Engineering Perspectives (AMOP 2025). – SPIE, 2025. – V. 14014. – P. 83-89.
5. Soleimani H. M. Mechanistic Insights Economic Modeling and Research Priorities for Nanoparticle Assisted Enhanced Oil Recovery. – 2025.
6. Uzokov J., Mamaziyayeva S., Muxamadiev A., Ruziyev I., Mukhamadiev N.. Quantum chemical investigation of the photocatalytic activity of TiO_2 nanoclusters with different structures //Advanced Materials for Optics and Photonics: Chemistry and Engineering Perspectives (AMOP 2025). – SPIE, 2025. – V. 14014. – P. 111-116.
7. Malayalam Amarnath T. S. et al. Hybrid Electrospun Carbon Nanofiber/Bi2MoO6 Nanocomposites for Trace-Level Detection of Phenolic Aldehyde Vanillin in Food Samples //ACS Applied Nano Materials. – 2025. – V. 8. – №. 32. – P. 15916-15929.
8. Khodjayorova G. et al. Study of complex formation from s-triazine Cu (II) cation by quantum chemical method //AIP Conference Proceedings. – AIP Publishing LLC, 2024. – T. 3244. – №. 1. – C. 050027.
9. Ulugboyeva G. et al. Synthesis and texture characteristics of mesoporous silica //AIP Conference Proceedings. – AIP Publishing LLC, 2024. – V. 3244. – №. 1. – P. 050023.
10. Avazova N. S. Quantum Chemical Study of Variously Structural TiO_2 Nanoclasters with Photocatalytic Activity //Central Asian Journal of Medical and Natural Science. – 2025. – T. 6. – №. 1. – C. 81-87.
11. Abderrahmani A., Boukherroub R., Purnama I. Nanotechnology for Sustainable Agriculture, Environment, and Human Wellbeing //E3S Web of Conferences. – EDP Sciences, 2025. – V. 678. – P. 08002.
12. Zhan M. et al. Graphene oxide research: current developments and future directions //Nanomaterials. – 2025. – V. 15. – №. 7. – P. 507.
13. Xodjayorova G. et al. Quantum chemical study of the synthesis of a chilate complex based on Ni (II) cation and 1, 3, 5-tris-(betta oxoethyl) hexahydrooxo-s-triazine //Science and innovation. – 2024. – V. 3. – №. A3. – P. 75-82.
14. Hiremath A. et al. Facile Design of pani/g-cn/wo3 nanocomposites with Integrated Photocatalytic and Dielectric Functionalities //Journal of Physics and Chemistry of Solids. – 2025. – P. 113305.
15. Sun X. D. et al. Mesoporous silica modified zwitterionic poly (ionic liquids) with enhanced absorption for Cr^{3+} and dye as a tanning agent //Microporous and Mesoporous Materials. – 2025. – V. 396. – P. 113742.
16. Xu B. et al. Multifunctional mesoporous silica nanoparticles for biomedical applications //Signal transduction and targeted therapy. – 2023. – V. 8. – №. 1. – P. 435.
17. Buglak A. A., Ramazanov R. R., Kononov A. I. Silver cluster–amino acid interactions: a quantum-chemical study //Amino Acids. – 2019. – V. 51. – №. 5. – P. 855-864.
18. Gatteschi D., Sessoli R. Quantum tunneling of magnetization and related phenomena in molecular materials //Angewandte Chemie International Edition. – 2003. – T. 42. – №. 3. – C. 268-297.
19. Martin A. D. et al. Hirshfeld surface investigation of structure-directing interactions within dipicolinic acid derivatives //Crystal Growth & Design. – 2015. – V. 15. – №. 4. – P. 1697-1706.
20. Herchel R. et al. Experimental and theoretical investigations of magnetic exchange pathways in structurally diverse iron (III) Schiff-base complexes //Inorganic Chemistry. – 2015. – V. 54. – №. 17. – P. 8625-8638.

SAMARQAND DAVLAT UNIVERSITETI ILMIY AXBOROTNOMASI

НАУЧНЫЙ ВЕСТНИК SCIENTIFIC REPORTS

Texnik muharrir **Sh.Xoliqulov**

Muharrirlar:

I.Sulaymonov - fil.f.d., dotsent
E.Arziqulov - f.-m.f.d., dotsent
O.Yusupova - fil.f.n., dotsent

Mas'ul muharrir:

A. Sh. Yarmuxamedov - f.-m.f.n.

Muassis: Samarqand davlat universiteti Manzil: 140104,
Samarqand shahri, Universitet xiyoboni, 15.
Telefon: (0 366) 240-38-47, Faks: (0 366) 239-13-87 e-mail:
axborotnoma.uz
SamDU «Ilmiy axborotnoma» jurnali tahririyati kompyuterida terildi. Bosishga 30.03.2026-yilda ruxsat etildi. Qog'oz o'lchami A-4. Nashriyot hisob tabog'i 10,00
Buyurtma raqami 833. Adadi 30 nusxa.

ISSN 2181-1296